Neural indices of attention and distraction during visual search

by

Shengkai Zhao

5/10/2023

A thesis submitted to the
faculty of the Graduate School of
the University at Buffalo, The State University of New York
in partial fulfillment of the requirements for the
degree of

Master of Science
Neuroscience Program

Acknowledgements

I am sincerely grateful to my supervisor, Dr. Thomas J. Covey, for his invaluable support and guidance throughout my postgraduate journey. His mentorship has been instrumental in helping me overcome numerous challenges and persevere in completing my master's degree. I would also like to express my deepest gratitude to Dr. David W. Shucard and Dr. Sarah F. Muldoon, members of my dissertation committee, for their insightful feedback and contributions to my research.

I extend my heartfelt appreciation to the dedicated staff and fellow students at the University at Buffalo, who have provided me with immense assistance and created a nurturing academic environment. It is through their support that I have been able to enjoy two fulfilling and joyous years at the University at Buffalo.

As I embark on the next phase of my journey, I will cherish the memories of my time at the University of Buffalo. I am committed to continuing my efforts and striving for excellence, with the aspiration to make meaningful contributions to my alma mater and society at large.

Abstract

Visual search involves detecting perceptual features that constitute target objects while simultaneously ignoring non-target stimuli. The ability to identify relevant information among irrelevant distracting stimuli is critically important for effective decision-making and goal-directed behavior. The present study aimed to identify neurophysiological indices of target identification and distraction during visual search performance. Forty healthy participants completed a visual search task in which they had to determine if a target letter "F" was right-side up (2/3 of all trials, frequent target) or flipped upside down (1/3 of all trials, infrequent target). Electroencephalographic (EEG) data were obtained during the task, and event-related potential (ERP) indices of brain function were derived at multiple stages of information processing. Analyses focused on the P2, N2, and P3 components of the ERP waveform, which have peak amplitudes at approximately 200, 200-300, and 300-500 msec post-stimulus, respectively. Localization of the cortical sources of ERP component activity was also investigated using the standardized Low Resolution Electromagnetic Tomography (sLORETA) approach. The results indicated that there was enhancement of amplitude at frontal scalp electrodes for the P2 and P3 components during trials with high interference distraction, compared to trials with low interference distraction. This finding suggests greater involvement of executive neural systems, at both early and later stages of information processing, when there is a need for filtering highly distracting information. There was enhancement of N2 component amplitude during trials with infrequent targets, or when there was high interference distraction, in comparison to trials with frequent targets and low interference

distraction. This indicates that the N2 component is modulated when there is stimulus information that produces more complex visual search (i.e., conflict monitoring function of the N2). The findings provide insight into the neural activity associated with different stages of visual search performance. Engagement of executive control related to the filtering of distracting non-target stimuli is engaged within 200 msec after the onset of a complex visual stimulus array (P2 effect). Mechanisms related to the resolution of conflict that may exist either/both in the target and non-target stimuli are engaged within 200-300 msec post-stimulus (N2 effect), and a second pass attentional control process that likely enables target stimulus categorization is engaged at approximately 300-500 msec post-stimulus (P3 effect). Cortical source analysis using the sLORETA approach indicated that these mechanisms are likely enabled by a distributed cortical network with activity that is most pronounced in frontal and parietal brain regions.

Table of Contents

Introduction

Visual search is required when an individual has to scan the visual environment to find a particular object or target that may be embedded among other distracting objects (Treisman & Gelade, 1980). This process often requires the brain to process a high volume of incoming information, and to selectively allocate attentional resources in order to identify relevant information according to task-specific goals. There are several factors that could influence attention allocation, including physical salience of incoming information (Theeuwes, 2010), current goals (Folk & Remington, 2006), and multiple memory systems (Awh et al., 2012; Hutchinson & Turk-Browne, 2012). Visual search is applied across a variety of different environments for various purposes in daily life and work. For example, an efficient visual search strategy is essential for air traffic control specialists (Palma Fraga et al., 2021). Visual search also plays a crucial role in various aspects of daily life, such as locating individuals in crowded environments, identifying relevant information while browsing the internet, and searching for desired products during shopping.

Attentional control and distractibility have both been established as core processes involved in complex visual search (Wolfe et al., 2005), but the neural processes and networks that underlie these components of visual search are still not well understood. The present study therefore aimed to identify the neural indices of attention and distraction during complex visual search, using a task that was designed to isolate these distinct aspects of visual search performance. The visual search task used in the present

study included trials with non-target information that was either highly distracting, or moderately distracting. Furthermore, sometimes the target was an infrequent, unfamiliar stimulus, whereas on the majority of trials the target was a frequently occurring, more familiar stimulus. This design allowed for the investigation of visual search processing under different conditions of target frequency, and when distraction was either high or moderate (a complete description of the visual search task is provided further in the methods below; see also Figure 1). Electroencephalographic (EEG) data were obtained during the visual search task, and event-related potentials (ERP) were then derived from these data. This approach enabled the isolation of neural performance that was associated with selective attention to visual targets and distraction during visual search.

Event related potentials (ERPs) provide a particularly useful method for investigating the neural processes that underly perception and attention (Woodman, 2010). ERPs are obtained from averaging the EEG signal that is recorded across multiple trials of a task, and which is time-locked to the onset of task stimuli. The ERP waveform therefore represents the brain activity associated with processing the discrete trial stimuli. The ERP waveform derived from single trial EEG data consists of a series of positive and negative deflections, which correspond to different components of the ERP reflecting distinct stages of information processing. The early components of the ERP, including P1, N1, and P2, typically occur within the first 100-200 milliseconds after stimulus onset. These components are primarily influenced by the physical characteristics of the stimulus and provide valuable information regarding attentional demands during initial sensory

processing (Key et al., 2005). Later occurring components (approximately 200-600msec after stimulus onset), such as N2 and P3 (or P3a and P3b), is considered to primarily reflect stimulus evaluation and categorization processes (Huster et al., 2013; Polich, 2007).

The distinct components of the ERP waveform can be modulated by a variety of task-specific parameters, and therefore this approach provides an opportunity to probe neural performance related to visual search at distinct stages of information processing. The P2 component, for example, is a positive deflection in the ERP waveform that typically peaks around 200 ms after the onset of a visual stimulus. It is thought to reflect early perceptual processing and is sensitive to the physical characteristics of the stimulus, such as stimulus size, shape, and contrast (Luck, 2014). Some studies have suggested that the P2 may also be modulated by attention, with larger P2 amplitudes observed for attended compared to unattended stimuli (Hillyard & Anllo-Vento, 1998). The N2 component is a negative deflection in the ERP waveform that typically peaks around 250 ms after the onset of a visual stimulus. It is thought to reflect attentional selection and interference control processes, and its amplitude is sensitive to the degree of conflict between competing stimuli (Luck, 2014). For example, in a visual task where participants had to search for a target among distracting stimuli, the N2 amplitude was larger for trials with high levels of stimulus interference and distraction (Sawaki & Luck, 2011). Prior work has also suggested that the N2 component is influenced by the orientation of the stimuli during visual search, including the orientation of letters. Specifically, when letters are presented upside-down, this stimulus configuration can elicit a larger N170 amplitude compared to when the same letters are presented upright (Rossion et al., 2003). The P3 component is a positive

deflection in the ERP waveform that typically peaks around 300-500ms after the onset of a visual stimulus. It is a well-known index of cognitive processing and has been associated with a variety of cognitive operations, including attention allocation, working memory, and decision-making (Polich, 2007). The P3 component has also been thought to reflect the process of stimulus-response translation or integration, which bridges the gap between stimulus processing and response execution (Pritchard et al., 1999; Verleger et al., 2005).

The P3 component is further considered to be comprised of at least two somewhat distinct subcomponents: P3a and P3b (Polich, 2007). P3a is typically observed in response to infrequent, unexpected, or salient stimuli, and is thought to reflect a neural orienting response to these stimuli. P3a is thought to reflect activity output of the anterior cingulate cortex and the prefrontal cortex, and has been linked to the detection of environmental changes and the allocation of attentional resources. P3b, on the other hand, is elicited by the processing of attended stimuli and has been linked to the updating of working memory representations. P3b is typically observed in response to target stimuli in visual search tasks, and its amplitude has been found to increase with increasing working memory load (Polich, 2007). The P3b component has been associated with the posterior parietal cortex, and has been linked to the allocation of attentional resources to task-relevant information and the updating of working memory representations (Polich, 2007; Soltani & Knight, 2000).

Compared to fMRI and some other common brain imaging tools, EEG has higher temporal resolution and relatively lower spatial resolution. However, the development of

EEG/ERP source imaging has provided a useful supplementary methodology to study the cortical sources of scalp EEG data. This approach models the cortical activity associated with the generation of ERP components using high-density electrode EEG systems and realistic head anatomical models. ERP Source imaging combines the EEG with modern brain imaging based head anatomical models (individual or template based models, see (Michel & Brunet, 2019). This approach has been used on a limited basis to evaluate neural performance during visual search previously. For example, Lorenzo-López et al. (2008) used the standardized Low-Resolution brain Electromagnetic Tomography (sLORETA) analyses for identifying cortical sources of ERP activity to investigate neural correlates of age-related visual search decline (Lorenzo-López et al., 2008).

The Present Study

The aim of the present study was to identify neurophysiological indices of target identification and distraction during visual search performance. To accomplish this aim, a visual search task was used that had three different trial types that targeted different aspects of visual search performance (as noted above; see also Methods section below). Healthy participants completed a visual search task in which they had to complete a button press response according to whether a target letter "F" was right-side up (2/3 of all trials, frequent target) or flipped upside down (1/3 of all trials, infrequent target). This target letter was embedded in a 6 x 6 letter array with distracting non-target letters. On some trials, the non-target distraction letters were perceptually dissimilar to the F target (low interference distraction trials), whereas on other trials the non-target distraction

letters were perceptually similar (“E” and “T” letter stimuli; high interference trials). EEG activity was obtained during task performance, and ERP measures for each trial type were obtained, which allowed us to evaluate neural correlates of visual search across different contexts, as outlined above. Cortical source activity underlying the ERP data was also investigated using the sLORETA approach. The purpose of the source analysis was to identify the cortical regions that were associated with any task-specific effects identified for each of the ERP components.

Based on prior work noted above, it was anticipated that P2 amplitude would be enhanced for trials that had the lowest level of interference (Up F trials with low interference distractors), because this component is associated with attention towards the target, which could be reasoned would be better with lower distraction (Hillyard & Anllo-Vento, 1998). It was predicted that N2 amplitude would be enhanced for trials that produced greater interference (Up F trial with high interference distractors, and Down F trials), given this component’s role in conflict monitoring (Huster et al., 2013). Finally, it was predicted that P3 amplitude would exhibit a more frontal-central enhancement for the Down F target trials of the task, in line with a more P3a-type of response that is often elicited for less frequent, unfamiliar targets (Polich, 2007).

Method

Participants

Forty-four normal, healthy young adults were entered into the study and completed the visual search task. Four of the participants had excessive noise/artifact in the EEG and were excluded from subsequent analyses, resulting in a total of forty participants in the final sample. The age requirement for participants was 20 to 35 years old. In the final sample of the visual search task group, 29 individuals were Caucasian, seven were Asian, two were African-American, one was Indigenous American, and one was Middle Eastern. Statistics for demographic characteristics are reported in the Results, and can be seen in Table 1. Participants were recruited via flyers posted at and around the University at Buffalo campuses. University at Buffalo IRB approval was obtained prior to the study.

Participant exclusion criteria for the study included a history of traumatic head injury, neurological disorder, cerebrovascular disease, major illness affecting cognition, learning disability, dementia, and substantial hearing or vision loss that could potentially interfere with the tasks involved in the study. Participants with alcohol or substance abuse or dependence, severe psychiatric disorders, or taking any neurological medications or steroids were also excluded from the study.

Table 1.

Participant demographics.

Variable	Statistic
Age in years, M (SD)	24.28 (4.04)
Gender:	
Female, n	30
Male, n	10
Years of Education, M (SD)	16.75 (1.84)
NAART estimated full scale IQ, M (SD)	108.38 (8.49)

Notes: NAART = North American Adult Reading Test; M = mean; SD = Standard Deviation; IQ = Intelligence Quotient

Visual search task

The visual search task utilized in this study was adapted from a task previously used by Redick et al (Redick et al., 2013), and was examined as part of a larger study on cognitive training (Covey et al., 2019). The task is depicted in Figure 1. During the task, participants focused on a central fixation cross displayed on the screen, followed by the presentation of a 6x6 array of letters in Courier New font located around the fixation cross for a duration of 1000 ms. The array contained only one target, which was either an upright 'F' or an upside-down, flipped 'F', while the remaining letters were distractors intended to interfere with target identification. The distractors were either low interference, meaning that they were perceptually dissimilar to the target F letter (A, C, D, M, S, X, and Y), or high interference, meaning that they were perceptually very similar to the target F letter due to shared stimulus features (E and T). This resulted in four distinct trial types: 100 trials with an Up F target and low interference distractors (44.4%); 65 trials with a Down F target and low interference distractors (28.9%); 50 trials with an Up F target

and high interference distractors (22.2%); and 10 trials with a Down F target with high interference distractors (4.4%). Each trial contained only three different letters (the F target, and then two different letters for the non-target distractors). Following the 1000ms stimulus presentation, a 1400ms inter-stimulus interval (ISI) was introduced that included a stimulus mask consisting of visual white noise to control for afterimage effects. Before the main test block there was a 5 min practice. During the presentation of the task stimuli, participants were comfortably seated in a chair positioned approximately 70 cm away from the computer monitor with the EEG net recording their brain activity during task performance in real time. The distance was measured from the participants' nasion to the screen. Participants registered their response with a button response pad during the test. They were required to press both the inner buttons with their two index fingers when they saw the Down F target, and press both the outer buttons with their two index fingers when they saw the Up F target.

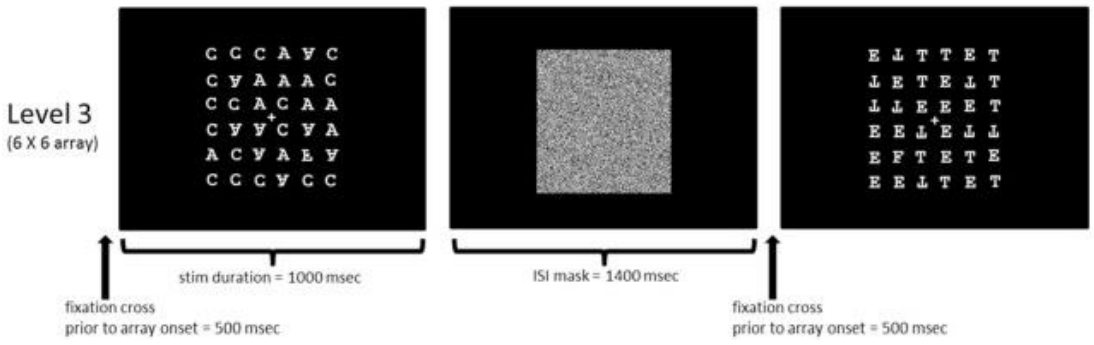

Fig. 1. The example depicts the presentation sequence of the visual search task blocks on the screen. The left panel displays an example of a Down F target with low interference distraction, while the right panel shows an example of an Up F target with high interference distraction. The middle panel represents the white noise presented between task blocks.

Electrophysiological measures

EEG recordings were obtained from participants seated in a quiet and controlled environment using a 256-channel dense electrode array HydroCel Geodesic Sensor Net (Electrical Geodesics, Inc., Eugene OR). Electrode impedances were maintained below 50 kΩ, and Cz was utilized as the reference electrode. Standard protocols, consistent with previous studies conducted in our laboratory (Covey et al., 2019), were employed for EEG acquisition, processing, artifact rejection, and signal averaging. The EEG data were filtered between 0.1 and 100 Hz during acquisition and digitized at a sampling rate of 250 Hz.

The EEG data were processed with Netstation version 5.4.2 (Electrical Geodesics, Inc. in Eugene, OR). A low-pass filter of 25 Hz was applied to the data before it was segmented into different trial types, including Up F Regular (i.e., low/regular distractors) trials, Down F regular (low/regular distractors only), and Up F Interference (i.e., high interference distractors) trials. The epoch window was 1050ms long, consisting of 150ms before stimulus onset (used as baseline) and 900ms after stimulus onset.

Data segmentation was followed by the application of artifact rejection procedures to identify and remove channels with poor quality. Channels were deemed bad if they exceeded specific criteria, including a threshold greater than 100 μV using a 40ms moving average across the entire segment, a threshold less than 1.0 μV in a window size of 200ms, or a threshold greater than 200 μV over the entire segment. Additionally, eye blink artifacts were detected using a threshold greater than 100 μV in a window size of 150ms, with a 40ms moving average and a blink duration extended by 5ms. Eye movement artifacts were identified using a threshold greater than 55 μV with a 40ms moving average

and a window size of 200 ms. If 20% of the segments in a channel were considered bad, the entire channel was marked as bad. Segments were labeled as bad if they contained more than 20 bad channels, an eye blink or eye movement artifact. Following automated artifact detection, each trial segment underwent visual inspection by the experimenter, and segments still containing artifacts were marked and excluded from subsequent averaging. Electrodes identified as bad were replaced with interpolated data from other scalp locations. Averaging was performed for each trial category, and the data were re-referenced using the average reference. Bad segments were excluded from the final averaged waveform, and baseline correction was applied to all averaged waveforms using the 150 ms time prior to stimulus onset. Participants with excessive artifact or insufficient trial count (less than 15 trials contributing to the ERP) were excluded from subsequent ERP analyses.

To categorize the scalp regions corresponding to conventionally used electrode locations (10-20 system), clusters of electrodes were defined. The study analyzed the following midline cluster regions: frontal (Fz), central (Cz), and parietal (Pz). ERP component amplitude and latency values were averaged across electrodes within three separate electrode clusters: frontal (seven adjacent electrodes), central (seven adjacent electrodes), and parietal (six adjacent electrodes). An automated algorithm was used to extract ERP values, selecting the highest peak within the defined window for each component (P2, N2, P3) and stimulus category, as determined from the grand average for each task. The window boundaries were visually inspected and adjusted if necessary to ensure the correct peak was being selected. Visual inspection of the grand averages

and peak selection were limited to the first 900ms post-stimulus (1050ms total) of the epoch.

ERP cortical source analysis

ERP cortical source data was obtained using the GeoSource tool in Netstation version 5.4.2. The standardized Low-Resolution brain Electromagnetic Tomography (sLORETA) was chosen as the method for source localization due to its demonstrated accuracy and robustness in previous ERP source analysis studies (Mulert et al., 2004; Pascual-Marqui, 2002). The finite difference model (FDM) was selected as the computation model for its ability to account for the anisotropic conductivities of brain tissues (Fuchs et al., 2002). The head model and brain space that was used to map the source activity data was based on the Montreal Neurologic Institute (MNI) brain. The 2 nm Atlas Man head model of MNI was used to generate the head model due to its high spatial resolution and accuracy in ERP Source localization (Güllmar et al., 2010). The source montage was selected through the utilization of the Gyri option in GeoSource. This method groups dipoles based on the major brain gyri, which is a widely recognized atlas for localizing brain sources (Mazziotta et al., 2001). The sampling time for selecting the source activity estimates for each component was determined by identifying the peak latency of each component for each participant, at the electrode cluster where the peak was maximal, and using these latencies to define the corresponding time point at which the source data were obtained. Thus, each participant had a set of separate source activity datasets which were obtained for each distinct ERP component that was evaluated in this study.

Statistical analyses

Accuracy and reaction time (RT) were measured for each participant in the visual search task. To examine differences in accuracy and RT across trial types, repeated measures ANOVAs with Trial Type as the factor were conducted, and post-hoc tests were carried out using paired t-tests. ERP amplitude and latency differences were examined using repeated measures ANOVAs, separately for amplitude and latency (e.g., using a Trial Type X Electrode Cluster design). Post-hoc analyses were completed with paired t-tests. Correlation analyses were also performed between accuracy, RT, ERP component amplitude, and latency. For each trial type and cluster of ERP data, separate correlation analyses were conducted.

To compare the activity in different brain areas between trial types, cortical source activity was averaged across all of the voxels within each separate gyrus, and paired t-tests were performed that compared the average gyrus activity, selected at each ERP component, across each set of search task trial types (e.g., Down F trials contrasted with Up F Regular trials). These analyses were corrected for multiple comparisons using the False Discovery Rate (Benjamini-Hochberg correction) method. The effect size for all of the paired contrasts was measured using Cohen's *d*. Heat maps and bar graphs that indicated the effect size for each of these contrasts for each separate cortical gyrus were generated to illustrate these effects.

Result

Behavioral measures

There were significant main effects of Trial Type for both task accuracy and RT (see Figure 1). Post-hoc analyses revealed that participants had significantly lower correct response percentage (performance accuracy, see Fig 1A) and higher average reaction time for correct responses (see Fig. 1B) for Up F Interference trials compared to Up F Regular and Down F Regular trials ($p<.001$). Down F Regular trials also had significant longer reaction time compared to Up F Regular trials, although these two trial types were not significantly different with respect to accuracy. These finding indicate that Up F Interference trials were generally the most challenging for the participants, in comparison to the other trial types, and that Down F Regular trials required additional processing time compared to the Up F Regular trials.

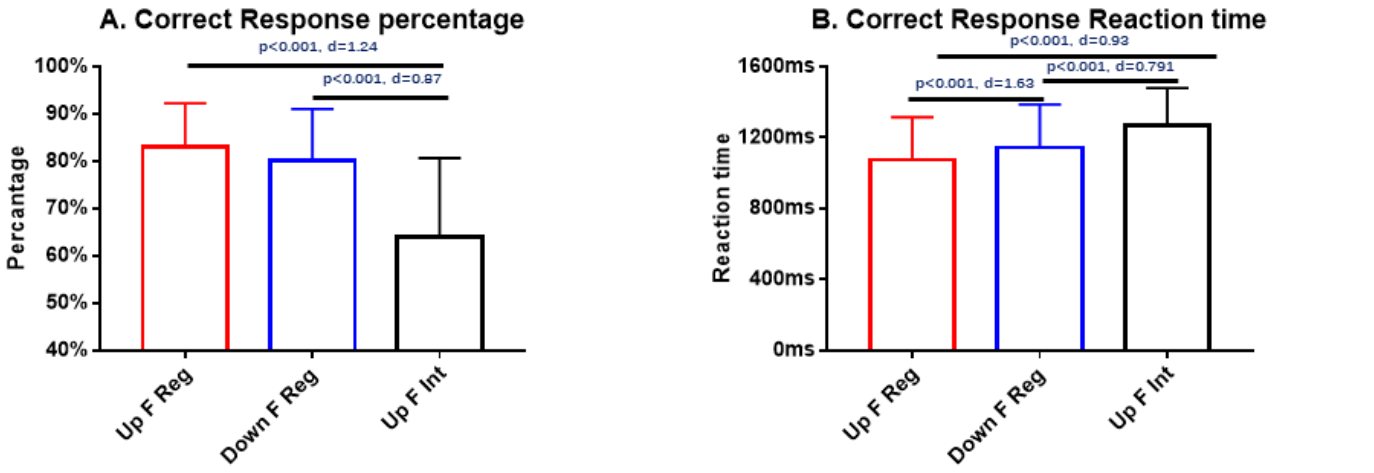

Fig. 2. Bars graphs display the percentage of correct responses for each trial type n Figure 2A, while Figure 2B shows the reaction time of correct responses after stimulus presentation for each trial type separately. Significant contrasts are indicated in each figure. Bars depict the mean and error bars indicate standard deviation of the mean. The effect obtained from the repeated measures ANOVA is also listed.

ERP Analyses

Figure 3 depicts the grand averaged ERP data obtained for the visual search task. The P2 component manifests as a positive peak in the waveform, typically observed at around 200 milliseconds (ms) with a frontal-central distribution across all electrodes. Similarly, the N2 component appears as a negative peak in the waveform, typically occurring between 200 and 300 ms, and exhibiting a more central distribution across all electrodes. Lastly, the P3 component is characterized by a positive peak in the waveform, typically observed between 200 and 300 ms, with a central-parietal distribution across all electrodes.

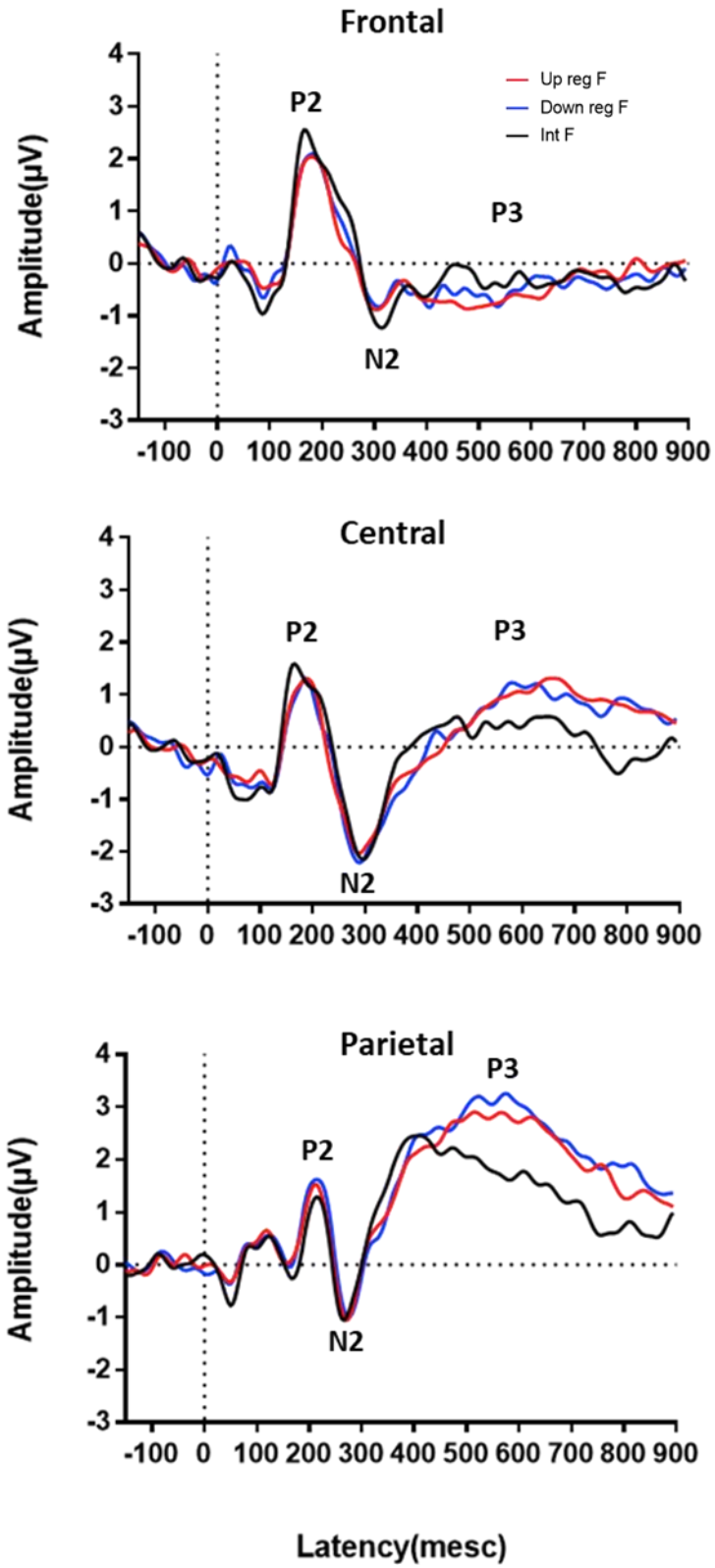

Fig. 3. The ERP waveforms of three distinct trial types at the Fz, Cz, and Pz electrodes are depicted in the top, middle, and bottom panels, respectively.

ERP Amplitude Analysis

There was a significant Trial Type X Electrode interaction for P2 amplitude (see Figure 4A). Post-hoc analyses indicated that Up F Interference trials had significantly larger frontal P2 amplitude compared to both the Down F Regular and the Up F Regular trials. A significant Trial Type effect was observed for the amplitude of the N2 component (see Figure 4B). Follow-up analyses revealed that Up F Interference trials exhibited significantly larger central P2 amplitudes compared to the Up F Regular trials. Furthermore, a significant Trial Type X Electrode interaction was found for the amplitude of the P3 component (see Figure 4C). Post-hoc analyses indicated that Up F Interference trials showed significantly larger frontal P3 amplitudes compared to the Up F Regular trials.

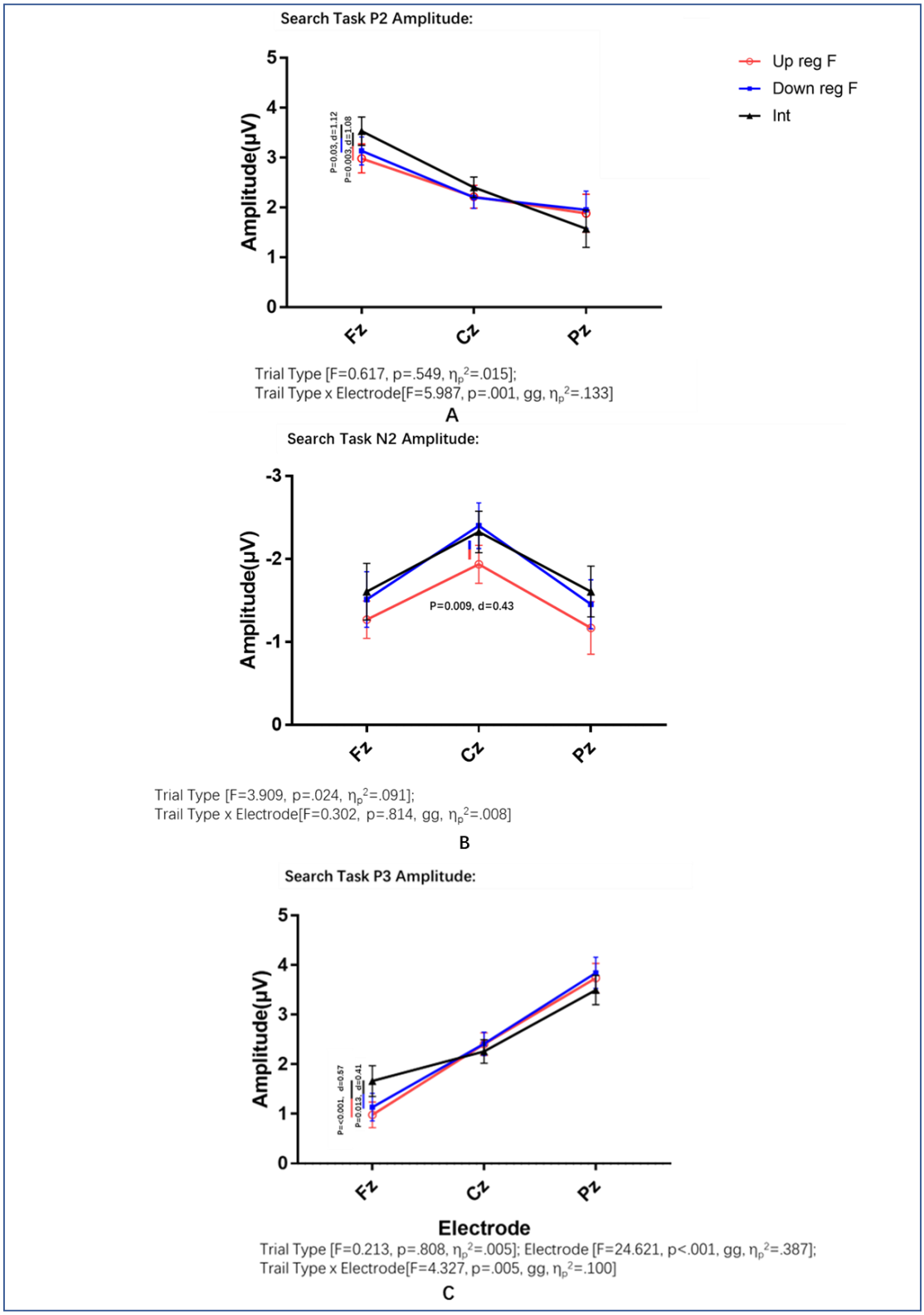

Fig. 4. Figure 4A and Figure 4C show the amplitudes of P2 and P3 components, and illustrate frontal enhancement for trials with high interference distraction. Figure 4B illustrates that the N2 amplitude at the Cz electrode was stronger for Up F targets with high interference distraction and Down F targets with low interference distraction, compared to Up F targets with low interference distraction.

ERP Latency Analysis

There were no significant interactions or Trial Type effects observed for P2 or N2 latency. There was a significant Trial Type X Electrode interaction for P3 latency. Post-hoc analyses indicated that P3 latency was significantly earlier for Up F Interference trials compared to both the Down F Regular and Up F Regular trials, at the Cz and Pz electrode locations. There was no significant difference between trial types at the Fz electrode.

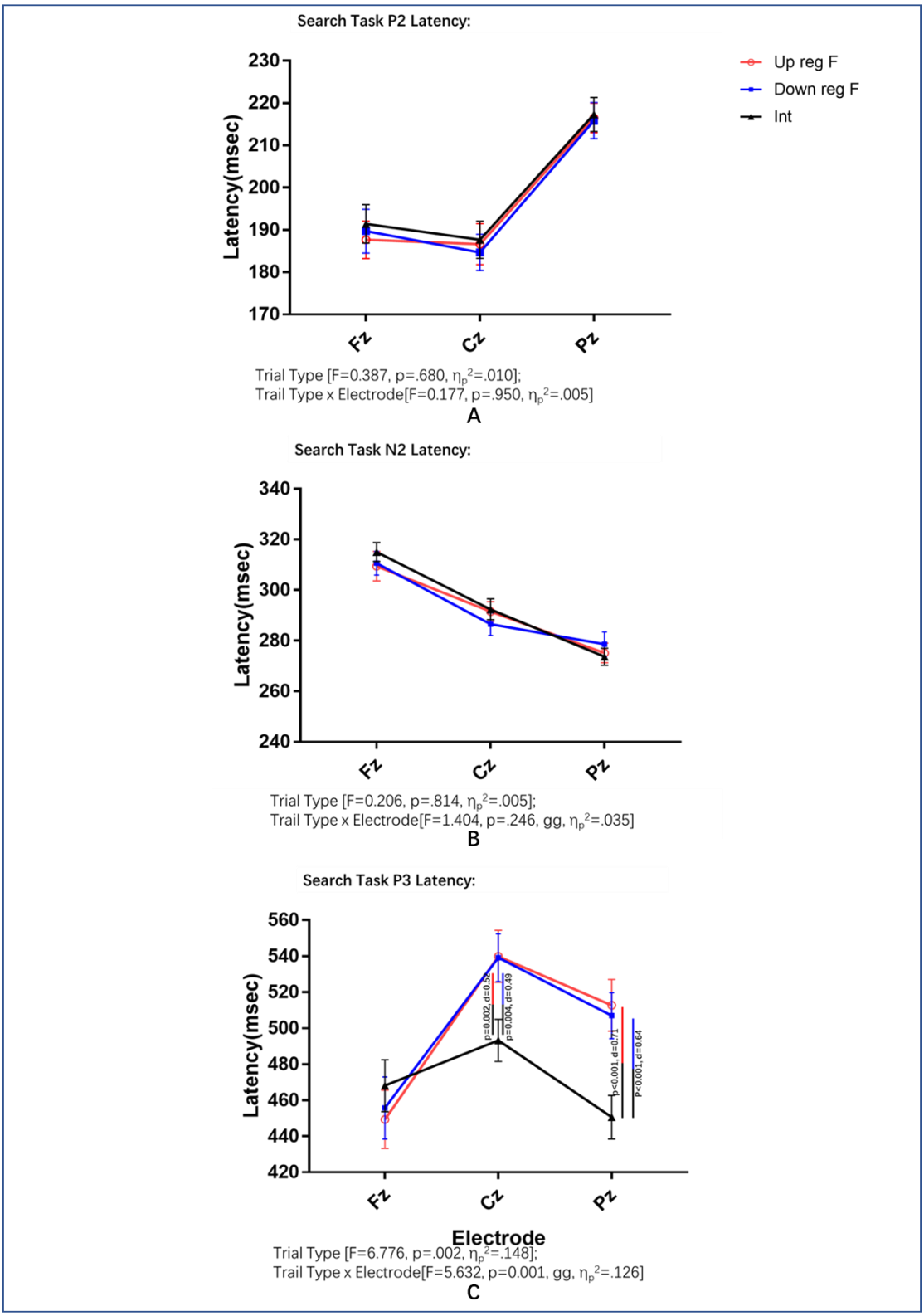

Fig. 5. Figure 5A displays the P2 latency at Fz, Cz, and Pz electrodes across three distinct trial types. Figure 5B depicts the N2 latency at Fz, Cz, and Pz electrodes across the same three trial types. Finally, Figure 5C illustrates the P3 latency at Fz, Cz, and Pz electrodes across the three trial types. It is noteworthy that the Up F target with high interference distraction trial exhibited a significantly faster latency at Cz and Pz compared to the other two trial types.

Relationships between behavioral performance and ERP measures

Pearson correlation analyses indicated that performance accuracy for the Up F Interference trials was significantly, and negatively, correlated with Pz amplitude of the P2 (r = -.430, p = .006) N2 (r = -0.323, p = 0.042) and P3 (r = -0.368, p = 0.010) (see table 2). Faster reaction time for Up F regular trials was significantly correlated with N2 latency at Cz (r = .339, p = .032) and Pz (r = .378, p = .016). Finally, Down F regular accuracy was significantly, and positively, associated with longer P3 latency at Fz (r = .378, p = .016) and Cz (r = .365, p = .021).

Table 2.

			P1 Amp Pz	N1 Amp Pz	P2 Amp Fz	P2 Amp Cz	P2 Amp Pz	N2 Amp Fz	N2 Amp Cz	N2 Amp Pz	P3 Amp Fz	P3 Amp Cz	P3 Amp Pz	P1 Lat Pz	N1 Lat Pz	P2 Lat Fz	P2 Lat Cz	P2 Lat Pz	N2 Lat Fz	N2 Lat Cz	N2 Lat Pz	P3 Lat Fz	P3 Lat Cz	P3 Lat Pz
Up F target with low interefence distraction	Correct reponse percentage	Pearson Correlation	0.035	0.033	0.120	0.114	-0.005	0.151	0.015	0.010	0.145	0.226	0.054	0.145	0.090	-0.102	-0.053	0.010	-0.025	-0.118	-0.009	0.083	0.035	-0.187
		Sig. (2-tailed)	0.831	0.840	0.460	0.483	0.976	0.352	0.925	0.952	0.371	0.162	0.740	0.373	0.579	0.530	0.746	0.952	0.876	0.468	0.956	0.611	0.830	0.249
	Reaction time	Pearson Correlation	0.162	0.163	-0.006	0.147	0.000	0.189	0.253	-0.041	0.209	0.124	-0.251	0.056	0.070	0.224	0.228	0.064	0.339	0.276	0.378	0.144	0.093	-0.068
		Sig. (2-tailed)	0.319	0.313	0.972	0.365	0.998	0.242	0.115	0.801	0.194	0.446	0.118	0.730	0.668	0.164	0.157	0.697	0.032*	0.085	0.016*	0.376	0.568	0.675
Down F target with low interefence distraction	Correct reponse percentage	Pearson Correlation	-0.087	-0.227	0.104	-0.158	0.043	-0.232	-0.405	-0.102	-0.003	0.108	0.164	0.119	-0.121	-0.153	0.030	0.015	0.024	0.062	-0.076	0.356	0.365	-0.107
		Sig. (2-tailed)	0.595	0.159	0.525	0.331	0.793	0.150	0.010*	0.530	0.986	0.507	0.313	0.463	0.455	0.346	0.855	0.925	0.881	0.703	0.641	0.024*	0.021*	0.509
	Reaction time	Pearson Correlation	-0.048	0.017	-0.059	-0.029	0.035	0.043	-0.032	-0.051	0.086	0.001	-0.173	-0.176	-0.186	0.084	0.122	-0.195	-0.068	0.026	-0.173	-0.129	0.175	-0.076
		Sig. (2-tailed)	0.767	0.917	0.717	0.858	0.832	0.794	0.846	0.754	0.599	0.996	0.287	0.277	0.252	0.607	0.454	0.228	0.677	0.873	0.284	0.426	0.281	0.643
Up F target with high interefence distraction	Correct reponse percentage	Pearson Correlation	-0.300	-0.379	0.273	-0.210	-0.430	0.061	-0.167	-0.323	0.263	-0.275	-0.368	-0.105	0.176	-0.183	-0.086	0.022	0.303	0.144	-0.054	0.167	-0.182	0.043
		Sig. (2-tailed)	0.060	0.016*	0.088	0.193	0.006*	0.706	0.304	0.042*	0.101	0.086	0.019*	0.518	0.278	0.259	0.599	0.892	0.057	0.375	0.742	0.304	0.262	0.794
	Reaction time	Pearson Correlation	0.019	0.042	0.035	-0.182	-0.063	0.180	0.099	-0.013	0.185	-0.038	-0.100	-0.053	0.133	0.234	0.277	-0.047	0.093	0.032	0.149	0.054	-0.080	-0.058
		Sig. (2-tailed)	0.909	0.799	0.831	0.262	0.699	0.265	0.542	0.936	0.252	0.818	0.538	0.747	0.414	0.146	0.083	0.775	0.570	0.844	0.358	0.740	0.624	0.724

Note: '*' marked the significant level of p<0.05.

ERP Source Analysis

In general, the ERP source analyses indicated that cortical activity was higher in magnitude for the Down F Regular trials compared to other trial types, and the Up F Interference trials exhibited higher magnitude cortical activity overall compared to the Up F Regular trials. Our analysis using Cohen's d values demonstrated that brain regions with the largest effect sizes were predominantly located in the frontal, parietal, and temporal lobes (refer to Figures 6-9 and Table 3). The statistical analyses conducted for the source analysis revealed significant brain regions that exhibited a contrast between conditions, while accounting for multiple comparisons. Brain regions that exhibited a statistically

significant contrast, while controlling for multiple comparisons, and which exhibited a large effect size for the pairwise contrast (d = .80) were flagged as robust indicators of between-trial contrasts. Table 3 provides a comprehensive list of the brain regions that reached statistical significance and exceeded the effect size threshold.

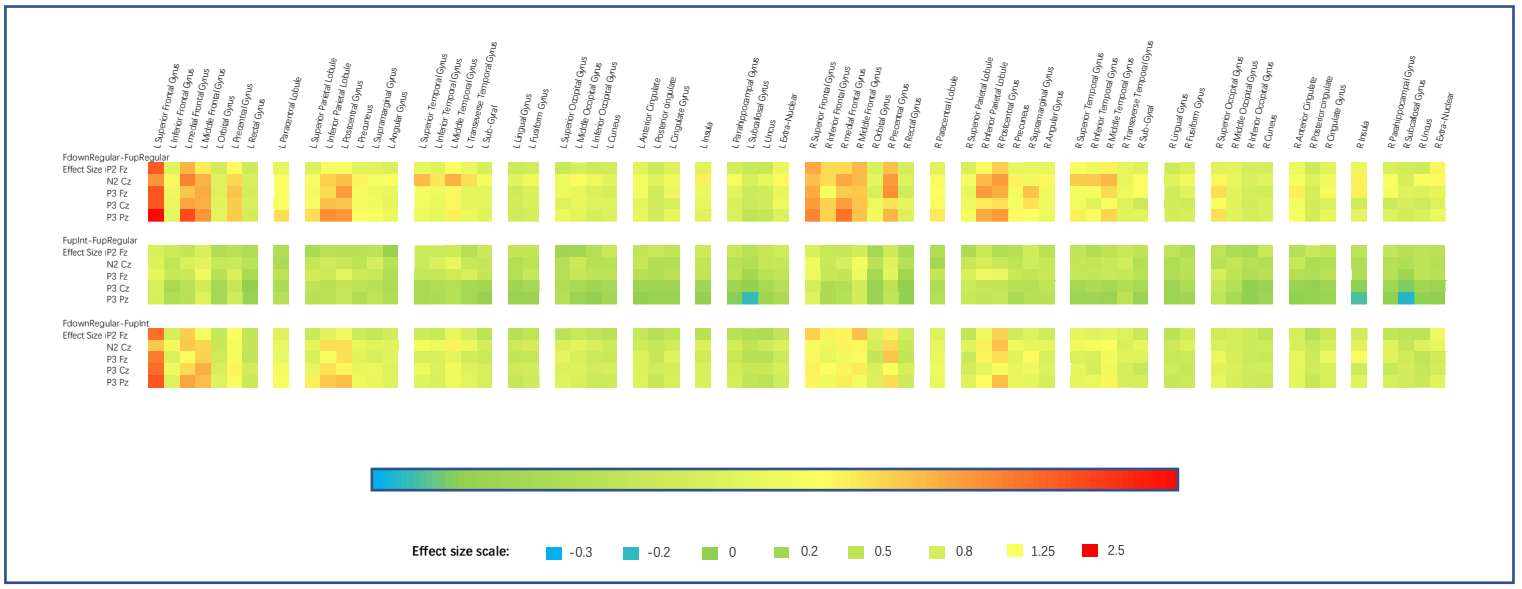

Fig. 6. In Figure 6, each block on the heat map represents a Cohen's d value between two different trial types for a specific ERP Source in a given brain area, with colors indicating the magnitude of Cohen's d. Scalp ERP effects and electrode locations that were identified as significant in the analyses above are shown on the leftmost column. The individual gyri are listed across the top of the figure.

Down F regular - Up F regular source activity contrast

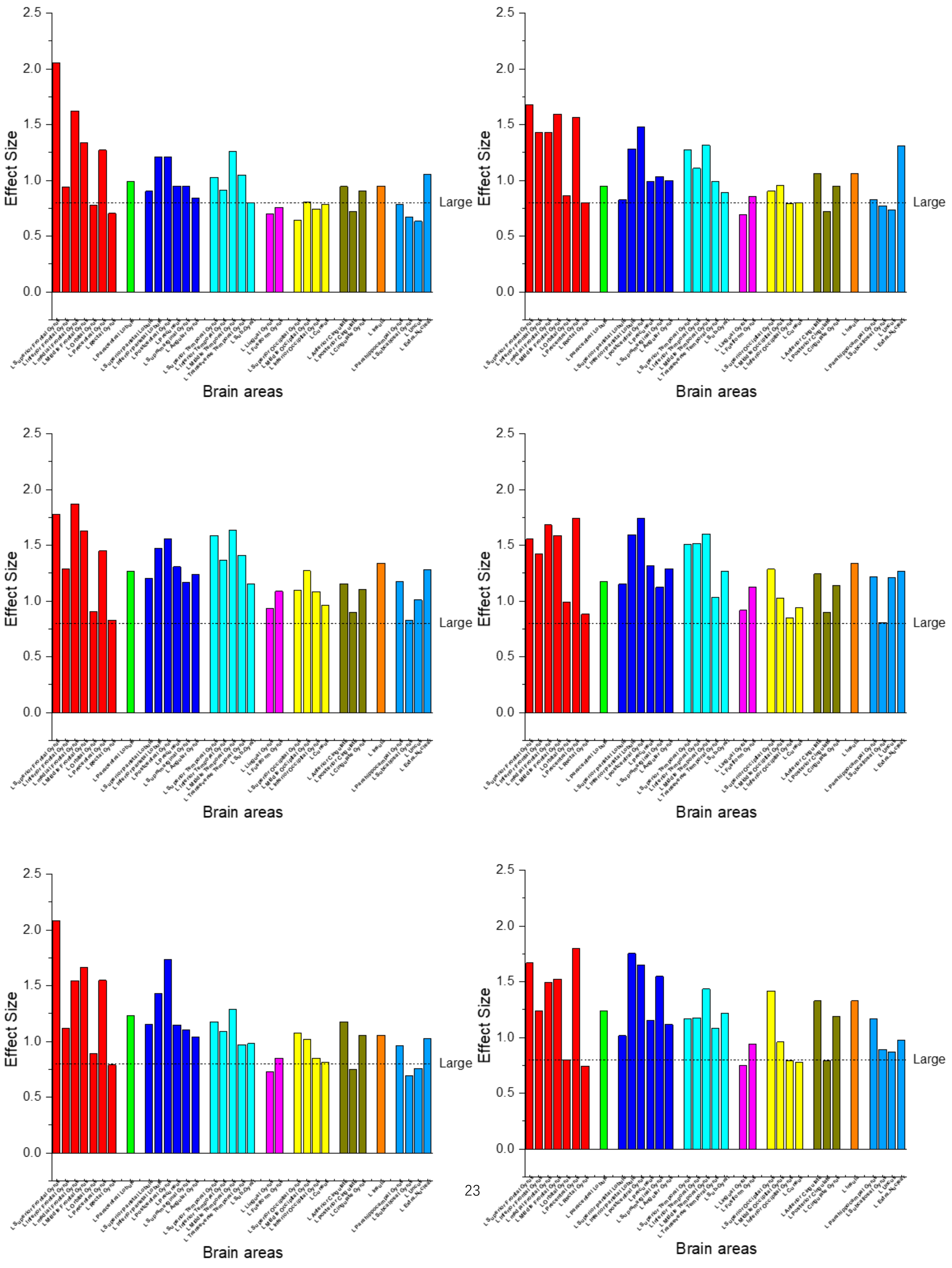

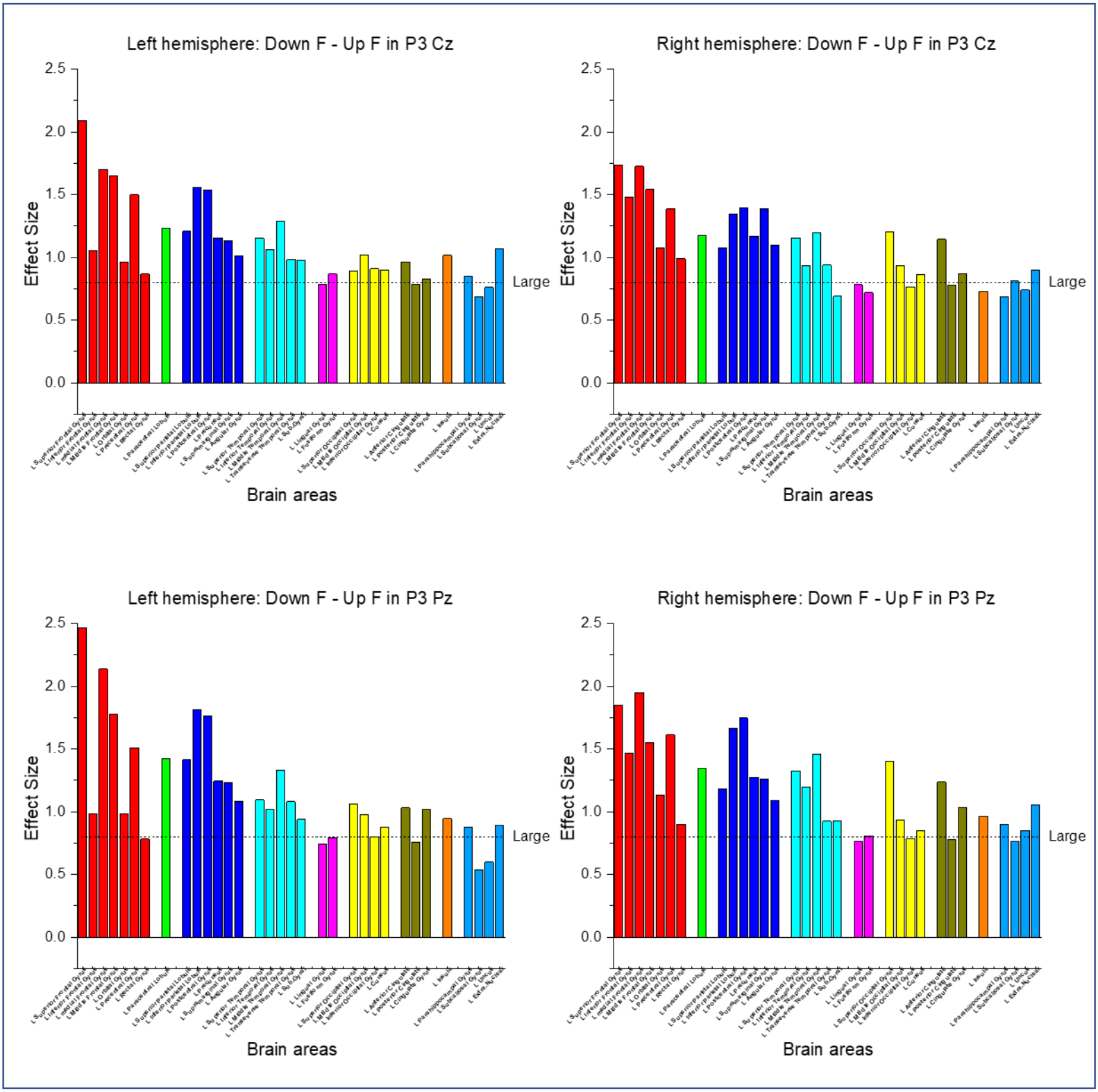

Fig. 7. The figure depicts the source localization contrast for Down F regular trials – Up F regular trials. In each figure, bar graphs depict the effect sizes measured by Cohen's d between trials featuring Down F target with low interference and Up F target with low interference in both the left and right hemisphere brain regions. The selection of the ERP Source data latency aligns with the latency of each of the ERP components described in the ERP analyses.

Up F Interference - Up F regular source activity contrast

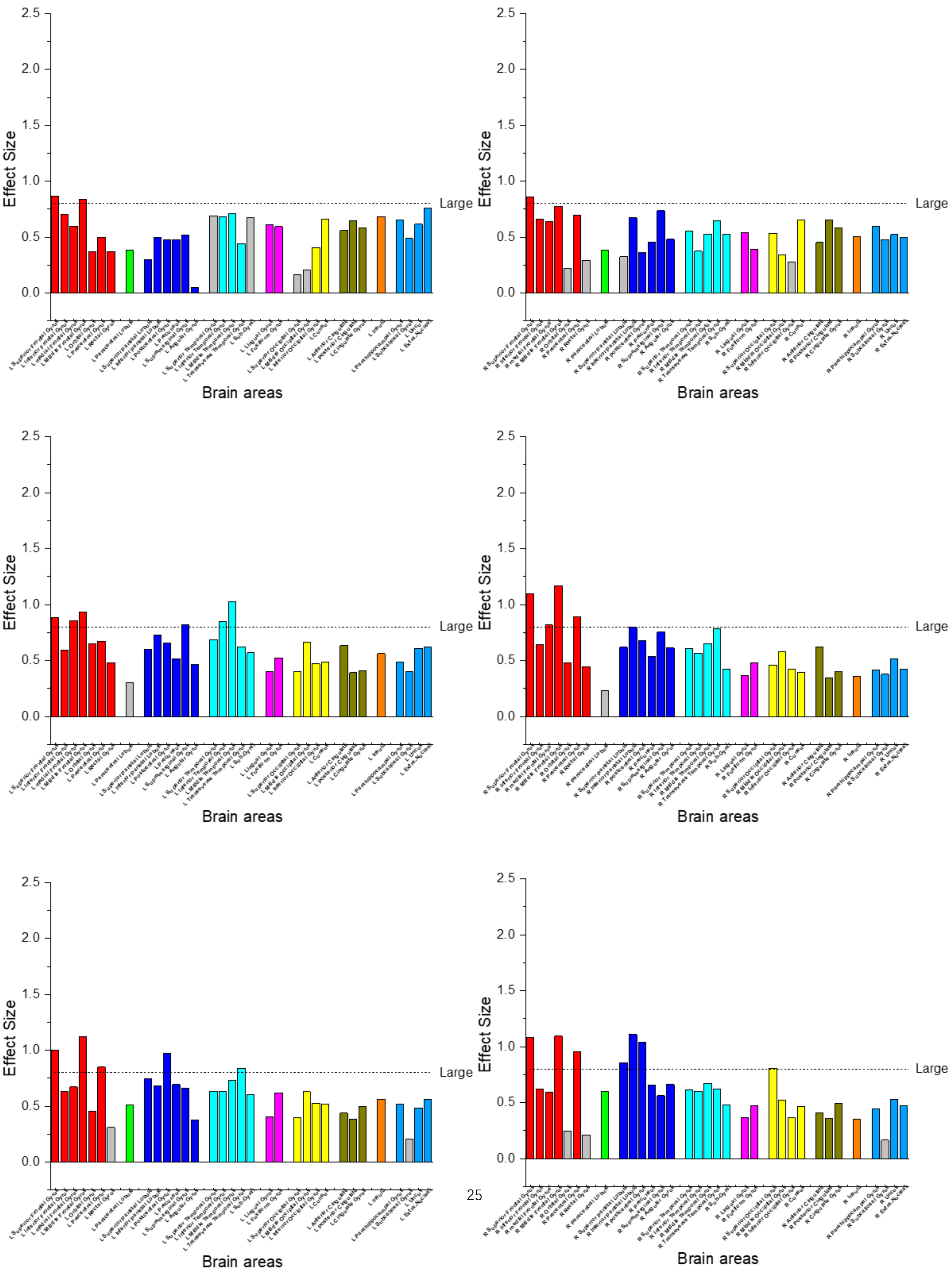

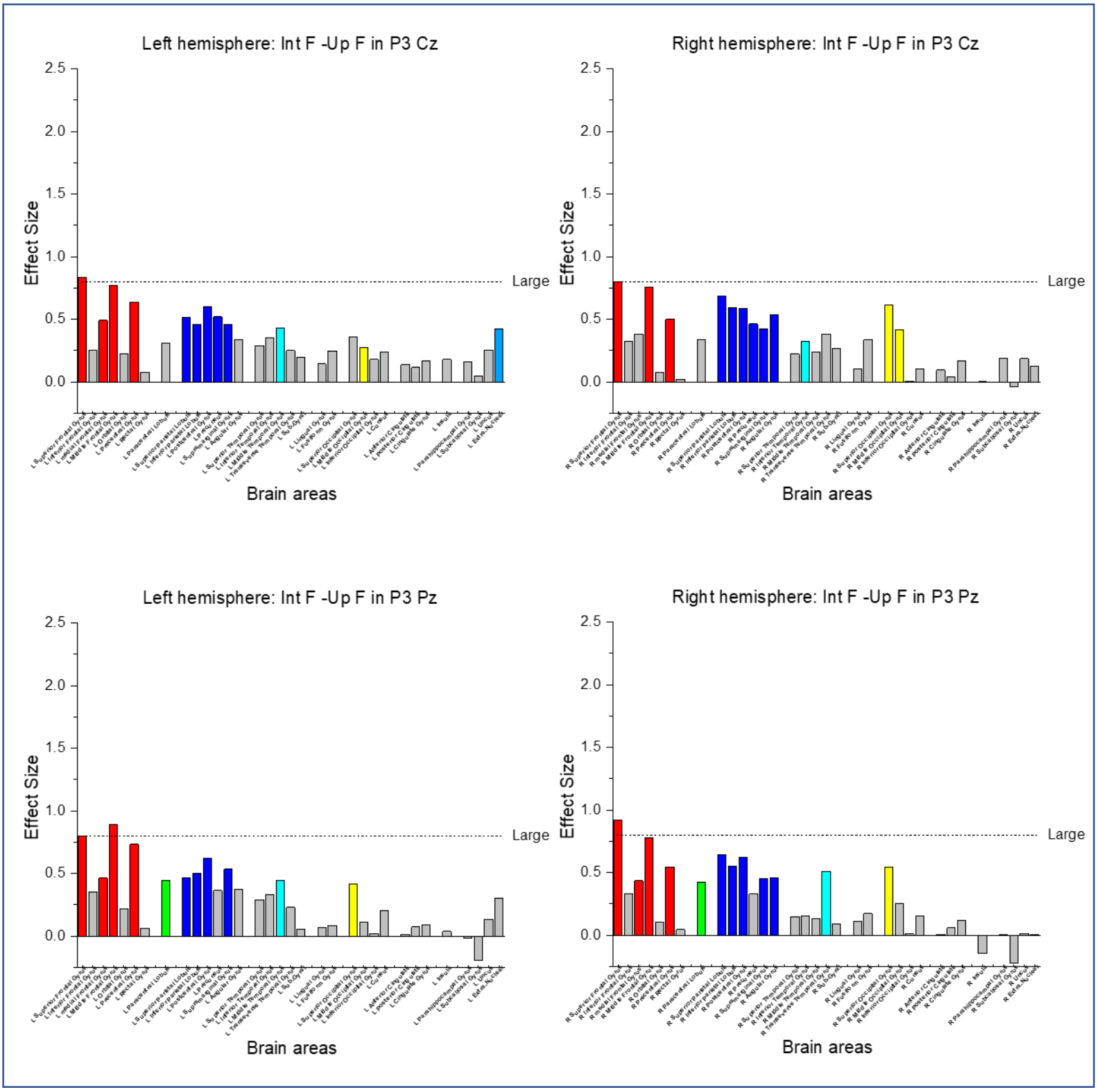

Fig. 8. The figure depicts the source localization contrast for Up F Interference trials – Up F regular trials. In each figure, bar graphs depict the effect sizes measured by Cohen's d between trials featuring Up F target with high interference and Up F target with low interference in both the left and right hemisphere brain regions. The selection of the ERP Source data latency aligns with the latency of each of the ERP components described in the ERP analyses.

Down F regular - Up F Interference source activity contrast

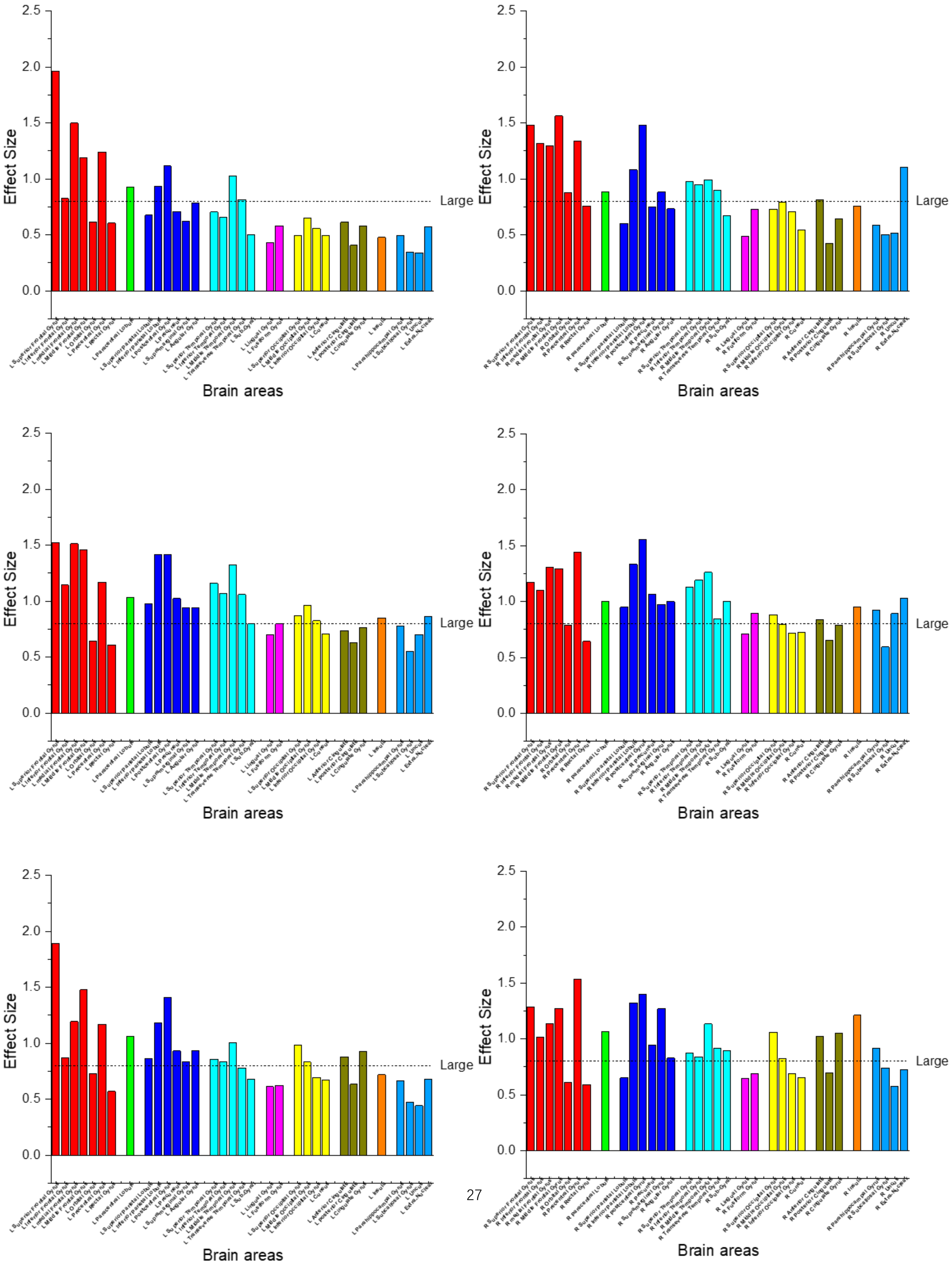

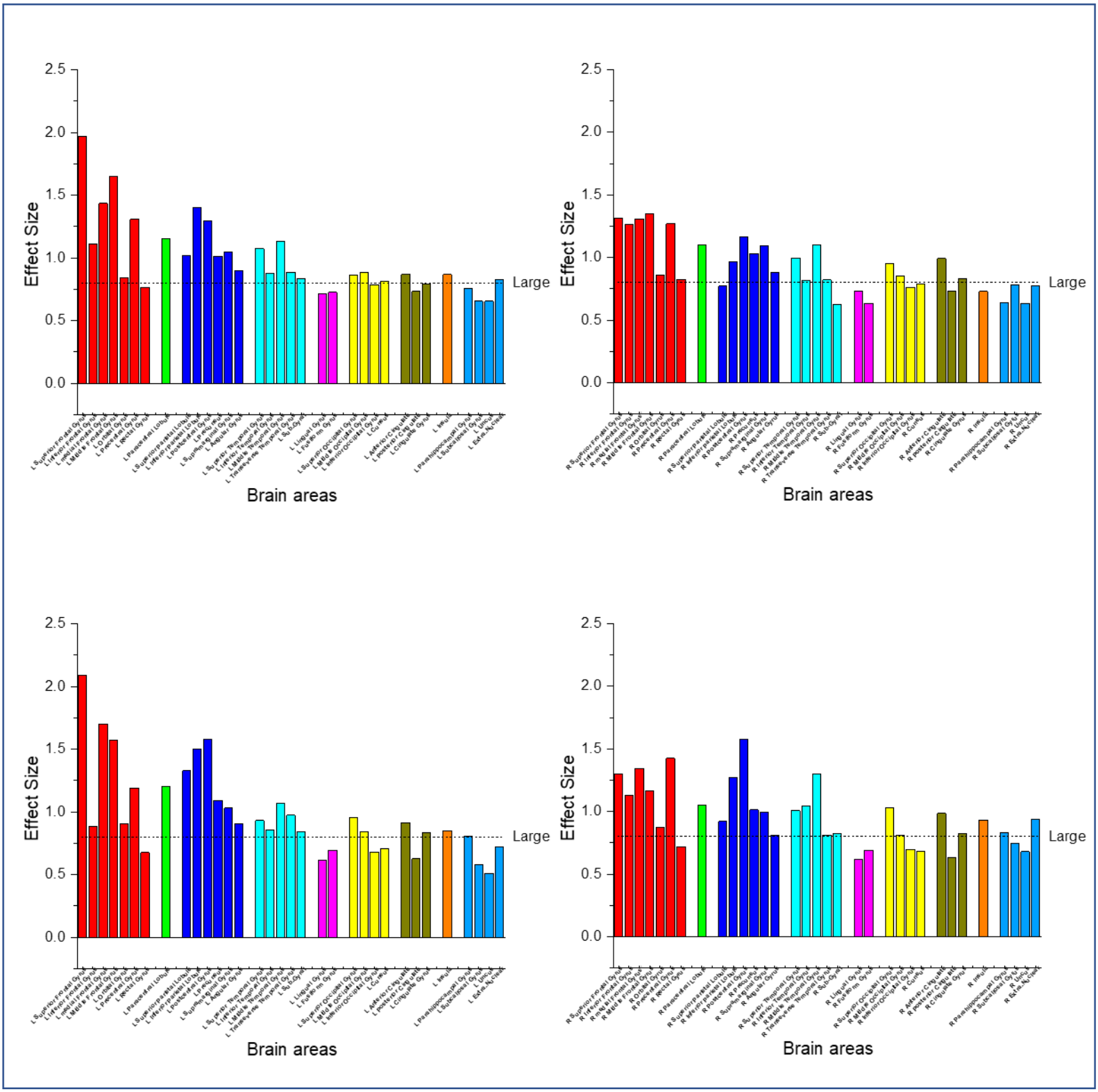

Fig. 9. The figure depicts the source localization contrast for Down F regular trials – Up F interference trials. In each figure, bar graphs depict the effect sizes measured by Cohen's d between trials featuring Down F target with low interference and Up F target with high interference in both the left and right hemisphere brain regions. The selection of the ERP Source data latency aligns with the latency of each of the ERP components described in the ERP analyses.

Table 3.

Regions exhibiting significance (p<0.05) and difference (d≥0.8)

	Left cerebral hemisphere	Right cerebral hemisphere	Bilateral cerebral hemispheres
FdownRegular > FupRegular			
P2 Fz		*Orbital Gyrus* *Fusiform Gyrus* *Superior Occipital Gyrus* *Parahippocampal Gyrus*	*Superior Frontal Gyrus* *Inferior Frontal Gyrus* *medial Frontal Gyrus* *Middle Frontal Gyrus* *Precentral Gyrus* *Paracentral Lobule* *Superior Parietal Lobule* *Inferior Parietal Lobule* *Postcentral Gyrus* *Precuneus* *Supramarginal Gyrus* *Angular Gyrus* *Superior Temporal Gyrus* *Inferior Temporal Gyrus* *Middle Temporal Gyrus* *Transverse Temporal Gyrus* *Sub-Gyral* *Middle Occipital Gyrus* *Anterior Cingulate* *Cingulate Gyrus* *Insula* *Extra-Nuclear*
N2 Cz			*Superior Frontal Gyrus* *Inferior Frontal Gyrus* *medial Frontal Gyrus* *Middle Frontal Gyrus* *Orbital Gyrus* *Precentral Gyrus* *Rectal Gyrus* *Paracentral Lobule* *Superior Parietal Lobule* *Inferior Parietal Lobule* *Postcentral Gyrus* *Precuneus* *Supramarginal Gyrus* *Angular Gyrus* *Superior Temporal Gyrus* *Inferior Temporal Gyrus* *Middle Temporal Gyrus* *Transverse Temporal Gyrus* *Sub-Gyral* *Lingual Gyrus* *Fusiform Gyrus* *Superior Occipital Gyrus* *Middle Occipital Gyrus* *Inferior Occipital Gyrus* *Cuneus* *Anterior Cingulate* *Posterior Cingulate* *Cingulate Gyrus* *Insula* *Parahippocampal Gyrus* *Subcallosal Gyrus* *Uncus* *Extra-Nuclear*
P3 Fz	*Orbital Gyrus* *Inferior Occipital Gyrus* *Cuneus*	*Subcallosal Gyrus* *Uncus*	*Superior Frontal Gyrus* *Inferior Frontal Gyrus* *medial Frontal Gyrus* *Middle Frontal Gyrus* *Precentral Gyrus* *Paracentral Lobule* *Superior Parietal Lobule* *Inferior Parietal Lobule* *Postcentral Gyrus* *Precuneus* *Supramarginal Gyrus* *Angular Gyrus* *Superior Temporal Gyrus* *Inferior Temporal Gyrus* *Middle Temporal Gyrus* *Transverse Temporal Gyrus* *Sub-Gyral* *Fusiform Gyrus* *Superior Occipital Gyrus* *Middle Occipital Gyrus* *Anterior Cingulate* *Cingulate Gyrus* *Insula* *Parahippocampal Gyrus* *Extra-Nuclear*
P3 Cz	*Inferior Occipital Gyrus* *Sub-Gyral* *Fusiform Gyrus* *Insula* *Parahippocampal Gyrus*	*Subcallosal Gyrus*	*Rectal Gyrus* *Orbital Gyrus* *Cuneus* *Superior Frontal Gyrus* *Inferior Frontal Gyrus* *medial Frontal Gyrus* *Middle Frontal Gyrus* *Precentral Gyrus* *Paracentral Lobule* *Superior Parietal Lobule* *Inferior Parietal Lobule* *Postcentral Gyrus* *Precuneus* *Supramarginal Gyrus* *Angular Gyrus* *Superior Temporal Gyrus* *Inferior Temporal Gyrus* *Middle Temporal Gyrus* *Transverse Temporal Gyrus* *Superior Occipital Gyrus* *Middle Occipital Gyrus* *Anterior Cingulate* *Cingulate Gyrus* *Extra-Nuclear*
P3 Pz	*Inferior Occipital Gyrus*	*Uncus* *Fusiform Gyrus* *Rectal Gyrus*	*Sub-Gyral* *Insula* *Parahippocampal Gyrus* *Orbital Gyrus* *Cuneus* *Superior Frontal Gyrus* *Inferior Frontal Gyrus* *medial Frontal Gyrus* *Middle Frontal Gyrus* *Precentral Gyrus* *Paracentral Lobule* *Superior Parietal Lobule* *Inferior Parietal Lobule* *Postcentral Gyrus* *Precuneus* *Supramarginal Gyrus* *Angular Gyrus* *Superior Temporal Gyrus* *Inferior Temporal Gyrus* *Middle Temporal Gyrus* *Transverse Temporal Gyrus* *Superior Occipital Gyrus* *Middle Occipital Gyrus* *Anterior Cingulate* *Cingulate Gyrus* *Extra-Nuclear*
FupInt > FupRegular			
P2 Fz	*Middle Frontal Gyrus*	*Superior Frontal Gyrus*	
N2 Cz	*Middle Frontal Gyrus* *Inferior Temporal Gyrus* *Middle Temporal Gyrus*	*Precentral Gyrus*	*medial Frontal Gyrus* *Middle Frontal Gyrus* *Superior Frontal Gyrus*
P3 Fz	*Middle Frontal Gyrus*	*Superior Parietal Lobule* *Inferior Parietal Lobule* *Superior Occipital Gyrus*	*Postcentral Gyrus* *Precentral Gyrus* *Middle Frontal Gyrus* *Superior Frontal Gyrus*
P3 Cz	*Superior Frontal Gyrus*		
P3 Pz	*Middle Frontal Gyrus*	*Superior Frontal Gyrus*	

FdownRegular > FupInt

P2 Fz				Orbital Gyrus Supramarginal Gyrus Superior Temporal Gyrus Inferior Temporal Gyrus Anterior Cingulate Extra-Nuclear
N2 Cz	Middle Occipital Gyrus Inferior Occipital Gyrus	Sub-Gyral Fusiform Gyrus Parahippocampal Gyrus Uncus Anterior Cingulate	Superior Parietal Lobule Precuneus Angular Gyrus Superior Occipital Gyrus Insula Supramarginal Gyrus Superior Temporal Gyrus Inferior Temporal Gyrus Extra-Nuclear Superior Frontal Gyrus Inferior Frontal Gyrus medial Frontal Gyrus Middle Frontal Gyrus Precentral Gyrus Paracentral Lobule Inferior Parietal Lobule Postcentral Gyrus Middle Temporal Gyrus Transverse Temporal Gyrus	Superior Frontal Gyrus Inferior Frontal Gyrus medial Frontal Gyrus Middle Frontal Gyrus Precentral Gyrus Paracentral Lobule Inferior Parietal Lobule Postcentral Gyrus Middle Temporal Gyrus Transverse Temporal Gyrus
P3 Fz	Superior Parietal Lobule	Sub-Gyral Parahippocampal Gyrus Insula Transverse Temporal Gyrus	Cingulate Gyrus Middle Occipital Gyrus Anterior Cingulate Precuneus Angular Gyrus Superior Occipital Gyrus Supramarginal Gyrus Superior Temporal Gyrus Inferior Temporal Gyrus Superior Frontal Gyrus Inferior Frontal Gyrus medial Frontal Gyrus Middle Frontal Gyrus Precentral Gyrus Paracentral Lobule Inferior Parietal Lobule Postcentral Gyrus Middle Temporal Gyrus	
P3 Cz	Cuneus Extra-Nuclear Superior Parietal Lobule Sub-Gyral Insula	Rectal Gyrus Cingulate Gyrus	Orbital Gyrus Transverse Temporal Gyrus Middle Occipital Gyrus Anterior Cingulate Precuneus Angular Gyrus Superior Occipital Gyrus Supramarginal Gyrus Superior Temporal Gyrus Inferior Temporal Gyrus Superior Frontal Gyrus Inferior Frontal Gyrus medial Frontal Gyrus Middle Frontal Gyrus Precentral Gyrus Paracentral Lobule Inferior Parietal Lobule Postcentral Gyrus Middle Temporal Gyrus	
P3 Pz		Extra-Nuclear	Parahippocampal Gyrus Superior Parietal Lobule Sub-Gyral Insula Cingulate Gyrus Orbital Gyrus Transverse Temporal Gyrus Middle Occipital Gyrus Anterior Cingulate Precuneus Angular Gyrus Superior Occipital Gyrus Supramarginal Gyrus Superior Temporal Gyrus Inferior Temporal Gyrus Superior Frontal Gyrus Inferior Frontal Gyrus medial Frontal Gyrus Middle Frontal Gyrus Precentral Gyrus Paracentral Lobule Inferior Parietal Lobule Postcentral Gyrus Middle Temporal Gyrus	

Discussion

The present study aimed to identify the distinct neural processes that are associated with target selection and the filtering of distracting non-target information during visual search performance. ERP component amplitude and latency were modulated in several important ways as a function of the variable parameters of the visual search task. P2 and P3 ERP components both showed enhancement of frontal amplitude when there were high interference distractors. N2 component amplitude was enhanced when there was any potential increased conflict in the stimulus parameters, such as when the target F was upside-down (more unfamiliar, less frequent), and when there were high interference distractors. Furthermore, central-parietal P3 amplitude tended to be earlier during trials with high interference distractors compared to other trial types. The interpretations of these findings, coupled with the source analysis findings, are described further below.

During visual search, different search processes or systems may be applied depending on the parameters of the stimuli. For example, a number of studies have suggested that parallel search and serial search are two types of search processes that can be applied differently depending on the type of interference distraction (Treisman & Gelade, 1980; Wolfe, 1994). Parallel search is thought to be engaged when the non-target information is substantially distinct from the target item in the visual stimulus array, and this process is completed fairly automatically. In contrast, serial search is more time consuming because the non-target stimuli in the array have overlapping features with the target stimulus, which requires a more deliberate, serial search through the stimulus

array to identify the target (Treisman & Gelade, 1980; Wolfe, 1994). This theoretical explanation of visual search could account to some extent for the findings of the present study, which observed that high distraction (i.e., on the Up F Interference trials) was associated with increased frontal P2 and P3 amplitude, lower accuracy, and longer RT. The behavioral findings indicated that Up F interference trial was the most difficult trial type for participants among the three trial types, and the increased frontal P2 and P3 amplitude may indicate greater executive demand for attention towards the target, as reflected by P2 (Potts, 2004), and target categorization, reflected by the P3 (Polich, 2007). This may be because high interference distraction ('E' and 'T') requires higher attentional resources to discriminate each letter one by one, compared to low interference distraction. In other words, participants may rely more on serial search in the Up F with high interference distraction trials and more on parallel search in the other two trial types with low interference distraction.

Prior studies have observed that N2 is functionally related to conflict monitoring and interference control processes (Sawaki & Luck, 2011). Furthermore, when letters are presented upside-down, a larger N170 amplitude can be elicited compared to when the same letters are presented in an upright orientation (Rossion et al., 2003). The findings of the present study indicated that N2 amplitude was enhanced for Up F Interference trials compared to Up F Regular trials, and a similar trend was observed for Down F Regular trials compared to Up F Regular trials. This is consistent with the prior work noted above that has observed, across separate studies, that the N2 is enhanced under conditions that produce conflict in task stimuli (i.e., Up F Interference) or if the target letter

is more novel or less familiar, such as when the targe letter is flipped upside down (i.e., Down F Regular). These collective findings point towards N2 as representing a generalized conflict resolution mechanism, which is engaged across a variety of situations and contexts when there is uncertainty or conflict in resolving stimulus features or stimulus-response mapping.

The findings of the present study also suggest that high interference distraction may have produced a shift in the relative influence of the P3a and P3b subcomponents in the overall P3 response. P3a is associated with the anterior cingulate cortex and prefrontal cortex and is related to the response to novel stimuli, while P3b is associated with the posterior parietal cortex and is linked to the allocation of attentional resources to task-relevant information and the updating of working memory representations (Polich, 2007; Soltani & Knight, 2000). The greater frontal P3 amplitude that was observed in the Up F target with high interference distraction trials suggests greater involvement of the P3a subcomponent in the ERP response relative to the other trial types in which the non-target stimuli were not as distracting. This is aligned with the notion of greater engagement of executive/frontal resources, which play a crucial role in tasks that require high interference control. Furthermore, it was also observed that central-parietal P3 latency was actually significantly earlier for the Up F Interference trials compared to other trial types, which was surprising. However, this may be further evidence of a distinct P3 subcomponent that is more similar to the P3a for the Up F Interference trials compared to the other trial types. The P3a response also tends to have an earlier latency and sharper peak compared to the later latency, broader morphology of the P3b (Polich, 2007). An

increased contribution of the P3a response during the Up F Interference trials may be required to resolve the interference produced by the highly distracting non-targets, and this may in turn facilitate subsequent processing of the target stimulus at a later point in time. It is possible that during the trials that do not have high interference distractors, there is greater involvement of the P3b overall, and this may reflect earlier onset of target stimulus categorization; whereas when the high interference distractors are present, there is greater involvement of P3a to resolve the conflict, or to engage serial search processes, and the target stimulus categorization may be further delayed. This possibility is consistent with the significant delay in behavioral response that was observed for the Up F Interference trials compared to the other trial types.

In the ERP source analysis, we observed higher cortical activity in the frontal, parietal, and temporal lobes for the Down F Regular trials compared to other trial types. The Up F Interference trials exhibited overall higher cortical activity than the Up F Regular trials, with the largest effect sizes predominantly located in these brain regions. The consistent large effects observed in the frontal areas align with the involvement of executive resources throughout the different stages of information processing in this task. It is possible that the lower magnitude of activity in the Up F Interference trials compared to the Down F Regular trials is due to a more focal and less distributed pattern of activation, which may be necessary for engaging in the type of serial search required by this condition.

It is worth noting that our study did not employ MRI to construct individualized head models for ERP source analysis. This limitation may have reduced the spatial resolution

of our findings. Future research could benefit from combining electrophysiological measures with MRI/fMRI to better identify the active brain regions during visual search tasks.

Given the relatively complex nature of the visual search task employed in our study, we observed greater variability in participants' performance, suggesting the utilization of various search strategies (such as serial and parallel search) and engagement of cognitive and memory systems. This complexity necessitates more intricate experimental designs and data analyses, but also enhances the relevance of our findings to real-world tasks.

Overall, our findings highlight the importance of frontal areas in visual search tasks, emphasize the potential benefits of multimodal neuroimaging approaches, and underscore the need to consider the complexity and variability inherent in such tasks for comprehensive experimental investigations. The findings point towards distinct neural processes associated with visual search. In particular, the present study indicates that the presence of highly distracting non-target information results in increased executive demand within 200ms after stimulus onset, and then again at approximately 300-500ms post-stimulus. Furthermore, conflict monitoring is engaged when either the non-target information is distracting, or the target is infrequent/unfamiliar.

Funding Acknowledgment: This work was supported in part by a pilot grant from the National Multiple Sclerosis Society.

Reference

Awh, E., Belopolsky, A. V., & Theeuwes, J. (2012). Top-down versus bottom-up attentional control: a failed theoretical dichotomy. *Trends Cogn Sci*, *16*(8), 437-443. https://doi.org/10.1016/j.tics.2012.06.010

Covey, T. J., Shucard, J. L., & Shucard, D. W. (2019). Working memory training and perceptual discrimination training impact overlapping and distinct neurocognitive processes: Evidence from event-related potentials and transfer of training gains. *Cognition*, *182*, 50-72. https://doi.org/10.1016/j.cognition.2018.08.012

Folk, C. L., & Remington, R. (2006). Top-down modulation of preattentive processing: Testing the recovery account of contingent capture. *Visual Cognition*, *14*(4-8), 445-465.

Güllmar, D., Haueisen, J., & Reichenbach, J. R. (2010). Influence of anisotropic electrical conductivity in white matter tissue on the EEG/MEG forward and inverse solution. A high-resolution whole head simulation study. *Neuroimage*, *51*(1), 145-163.

Hillyard, S. A., & Anllo-Vento, L. (1998). Event-related brain potentials in the study of visual selective attention. *Proceedings of the National Academy of Sciences*, *95*(3), 781-787.

Huster, R. J., Enriquez-Geppert, S., Lavallee, C. F., Falkenstein, M., & Herrmann, C. S. (2013). Electroencephalography of response inhibition tasks: functional networks and cognitive contributions. *Int J Psychophysiol*, *87*(3), 217-233. https://doi.org/10.1016/j.ijpsycho.2012.08.001

Hutchinson, J. B., & Turk-Browne, N. B. (2012). Memory-guided attention: control from multiple memory systems. *Trends Cogn Sci*, *16*(12), 576-579. https://doi.org/10.1016/j.tics.2012.10.003

Key, A. P., Dove, G. O., & Maguire, M. J. (2005). Linking brainwaves to the brain: an ERP primer. *Dev Neuropsychol*, *27*(2), 183-215. https://doi.org/10.1207/s15326942dn2702_1

Lorenzo-López, L., Amenedo, E., Pascual-Marqui, R. D., & Cadaveira, F. (2008). Neural correlates of age-related visual search decline: a combined ERP and sLORETA study. *Neuroimage*, *41*(2), 511-524.

Luck, S. J. (2014). *An introduction to the event-related potential technique*. MIT press.

Mazziotta, J., Toga, A., Evans, A., Fox, P., Lancaster, J., Zilles, K., Woods, R., Paus, T., Simpson, G., & Pike, B. (2001). A probabilistic atlas and reference system for the human brain: International Consortium for Brain Mapping (ICBM). *Philosophical Transactions of the Royal Society of London. Series B: Biological Sciences*, *356*(1412), 1293-1322.

Michel, C. M., & Brunet, D. (2019). EEG Source Imaging: A Practical Review of the Analysis Steps. *Front Neurol*, *10*, 325. https://doi.org/10.3389/fneur.2019.00325

Mulert, C., Jäger, L., Schmitt, R., Bussfeld, P., Pogarell, O., Möller, H.-J., Juckel, G., & Hegerl, U. (2004). Integration of fMRI and simultaneous EEG: towards a comprehensive understanding of localization and time-course of brain activity in target detection. *Neuroimage*, *22*(1), 83-94.

Palma Fraga, R., Kang, Z., Crutchfield, J. M., & Mandal, S. (2021). Visual search and conflict mitigation strategies used by expert en route air traffic controllers. *Aerospace*, *8*(7), 170.

Pascual-Marqui, R. D. (2002). Standardized low-resolution brain electromagnetic tomography (sLORETA): technical details. *Methods Find Exp Clin Pharmacol*, *24*(Suppl D), 5-12.

Polich, J. (2007). Updating P300: an integrative theory of P3a and P3b. *Clin Neurophysiol*, *118*(10), 2128-2148. https://doi.org/10.1016/j.clinph.2007.04.019

Potts, G. F. (2004). An ERP index of task relevance evaluation of visual stimuli. *Brain and cognition*, *56*(1), 5-13.

Pritchard, W. S., Houlihan, M. E., & Robinson, J. H. (1999). P300 and response selection: a new look using independent-components analysis. *Brain Topogr*, *12*(1), 31-37. https://doi.org/10.1023/a:1022277506517

Redick, T. S., Shipstead, Z., Harrison, T. L., Hicks, K. L., Fried, D. E., Hambrick, D. Z., Kane, M. J., & Engle, R. W. (2013). No evidence of intelligence improvement after working memory training: a randomized, placebo-controlled study. *Journal of Experimental Psychology: General*, *142*(2), 359.

Rossion, B., Joyce, C. A., Cottrell, G. W., & Tarr, M. J. (2003). Early lateralization and orientation tuning for face, word, and object processing in the visual cortex. *Neuroimage*, *20*(3), 1609-1624.

Sawaki, R., & Luck, S. J. (2011). Active suppression of distractors that match the contents of visual working memory. *Visual Cognition*, *19*(7), 956-972.

Soltani, M., & Knight, R. T. (2000). Neural origins of the P300. *Critical Reviews™ in Neurobiology*, *14*(3-4).

Theeuwes, J. (2010). Top-down and bottom-up control of visual selection. *Acta Psychol (Amst)*, *135*(2), 77-99. https://doi.org/10.1016/j.actpsy.2010.02.006

Treisman, A. M., & Gelade, G. (1980). A feature-integration theory of attention. *Cognitive Psychology*, *12*(1), 97-136. https://doi.org/https://doi.org/10.1016/0010-0285(80)90005-5

Verleger, R., Jaśkowski, P., & Wascher, E. (2005). Evidence for an integrative role of P3b in linking reaction to perception. *Journal of psychophysiology*, *19*(3), 165-181.

Wolfe, J. M. (1994). Guided Search 2.0 A revised model of visual search. *Psychonomic Bulletin & Review*, *1*(2), 202-238. https://doi.org/10.3758/BF03200774

Wolfe, J. M., Horowitz, T. S., & Kenner, N. M. (2005). Cognitive psychology: rare items often missed in visual searches. *Nature*, *435*(7041), 439-440. https://doi.org/10.1038/435439a

Woodman, G. F. (2010). A brief introduction to the use of event-related potentials in studies of perception and attention. *Atten Percept Psychophys*, *72*(8), 2031-2046. https://doi.org/10.3758/app.72.8.2031